

## NUMERICAL STUDY OF CAVITATING FLOW IN ASYMMETRICAL NOZZLES OF INJECTORS/ATOMIZERS. PART II. APPLICATION TO FULLY DEVELOPED CAVITATION CASES

**Miguel G. Coussirat, Flavio H. Moll**

*Laboratorio de Modelado Aeroelasticidad (LaMA), Universidad Tecnológica Nacional (UTN),  
Facultad Regional Mendoza (FRM), Argentina, [miguel.coussirat@frm.utn.edu.ar](mailto:miguel.coussirat@frm.utn.edu.ar),  
[flavio.moll@docentes.frm.utn.edu.ar](mailto:flavio.moll@docentes.frm.utn.edu.ar) <http://www.frm.utn.edu.ar>*

**Keywords:** Developed Cavitation; Injectors; Atomizers; Turbulence; Eddy Viscosity Models; Validation/Calibration.

**Abstract:** In the first part of this work a broad discussion related to steady and unsteady state cavitation cases and the calibration of turbulence models in steady state cases simulations was presented. In this second part, a numerical analysis of the unsteady flow behavior in nozzles of injectors/atomizers is presented. Previous works showed that it is possible to capture several of the incipient cavitating flow characteristics performing a careful calibration of the Eddy Viscosity Models in nozzles. This work extends the numerical study for these nozzles in cases where the fully developed cavitation state appears. Again, a careful calibration of the selected Eddy Viscosity Models becomes an important task to obtain accurate predictions of the flow. The results obtained show that it is possible to capture the main cavity features and the characteristic frequencies of the flow unsteadiness. The obtained conclusions could be useful to improve injectors design using numerical modeling, because the detection of the typical frequencies related to the flow unsteadiness could be useful to detect possible coupling between some of these frequencies and one of the natural vibration modes of the nozzle leading to a possible undesired fluid- structure interaction.

### 1. INTRODUCTION

In the first part of this work the general strategy used for steady state cavitating flow simulation in nozzles was discussed. This strategy included a detailed Eddy Viscosity Model (EVM) calibration. To simulate the fully developed cavitation cases, a set of experimental evidence compiled was also presented. The methodology applied and checked in steady state cases simulations is applied and extended to transient/unsteady simulations for fully developed cavitating flows in this second part of the work. Like in the first part of the work, the simulations are related to developing cavitating flows in low pressure Diesel injectors with an asymmetrical nozzle inlet configuration and square sections at the outlet. It is considered that the flow in the nozzle is under transient flow conditions, (slightly developed cavitation and fully developed cavitation states, i.e.,  $1.19 > \sigma > 0.94$ , see Fig. 1). The main subject here is to obtain a better performance of URAS+EVMs developed for general usage when they are applied to design devices where developing cavitating flows appear. Previous works showed that a careful EVM calibration is necessary, and it must rely on a physical basis. Conclusions obtained from Coussirat et al., 2016-2021 for steady cavitating flow simulations were presented and discussed in the first part of this work and will be a useful tool for performing the URAS+EVMs CFD simulations here.

### 2. EXPERIMENTAL DATABASES USED

A broad discussion of the used databases was made in the first part of this work. It was pointed out that, commonly, the cavitation states shown, Fig. 1 are classified by a two characteristic numbers, i.e., Reynolds, Re, and Cavitation,  $\sigma$ , K, numbers respectively, computed by the Eq. 1.

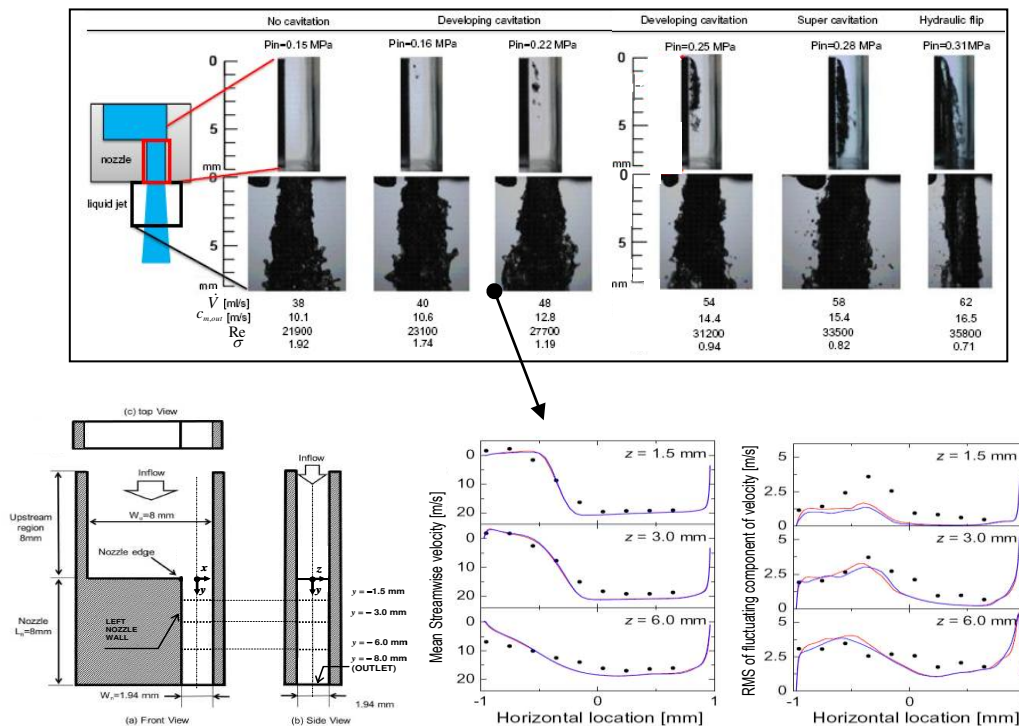


**Figure 1.** Geometry, experimental and CFD mean  $c_m$  and RMS fluctuating  $c'_{RMS}$  velocity profiles, for Reynolds number,  $Re = 27,700$ . Notation:  $\sigma$ , K, Cavitation numbers; Re, Reynolds number, see Eq. 1. ●, Experiments (LDV); CFD Smagorinsky (Red) and Vreman (Blue) LES SGS models respectively, Sou et al., 2014 and Biçer 2015. Equivalence ( $\sigma$ , K): (1.92, 3,00); (1.19, 1,83); (0.94, 1,66)

It was already mentioned that there are several stages into the developing cavitation state. A quasi-steady case ( $\sigma=1.74$ ) without vortex shedding and an incipient unsteady case that shows some vortex shedding evidence ( $\sigma=1.19$ ). The attention is focused now on the developing cavitation cases (i.e,  $\sigma = 1.19$  and  $\sigma = 0.94$ ) where the unsteady behavior is more relevant. Comparisons between previous steady state CFD simulations and the unsteady state ones performed now will be presented next.

The Eq. 1 was already presented in the first part of the work too, and it is reproduced here again for clarity in the discussion of the obtained results.

$$\begin{aligned} \text{Re} &= c_{m,out} w_n / \nu; \quad \text{We} = \rho c_{m,out}^2 t h_n / \tau_s; \quad \text{Sr} = f_{vs} L_{cav} / c_{m,out} \\ \sigma &= (p_{out} - p_v) / (0.5 \rho c_{m,out}^2); \quad \text{K} = (p_{out} - p_v) / (p_{in} - p_{out}); \end{aligned} \quad (1)$$

Being We and Sr, the Weber and Strouhal number respectively;  $w_n$ ,  $L_n$ ,  $t h_n$ , nozzle width, length and thickness respectively;  $c_{m,out}$ , outlet mean velocity;  $f_{vs}$ , vortex shedding frequency;  $\nu$ , liquid viscosity ( $=1.035 \times 10^{-6} \text{ m}^2/\text{s}$ );  $\rho$ , liquid density ( $=998 \text{ kg/m}^3$ );  $p_{in}$ , inlet pressure;  $\tau_s$ , surface stress ( $=7.28 \times 10^2 \text{ N/m}$ );  $p_{out}$ , outlet pressure ( $=1.0 \times 10^5 \text{ Pa}$ );  $p_v$ , vapor pressure ( $=2,300 \text{ Pa}$ );  $L_{cav}$ , cavity mean length.

### 3. METHODOLOGY DEVELOPED FOR URAS/EVM+TEM MODELING

In the first part of this work, it was discussed that the EVM calibration is as important as the derivation of the model itself. Calibration is achieved with the help of experimental and validated CFD results of the flow that should be modeled. The calibration process is also the first step in which the range of validity of the model would be checked by a detailed inspection and not just by its initial physical model definition. The previous works were related to calibrate EVMs in nozzles with flows under incipient cavitation, i.e., steady state. The studies consisted in EVMs and TEMs calibrations by means of careful parameters selection/tuning, joined to a mesh sensitivity study (Coussirat et al., 2016-2021). The parameters selection must be performed considering the close relation between the cavitation state and the turbulence kinetic energy,  $k$ , level in the flow considering the characteristics of detached flows. The followed methodology to guarantee accurate results was developed in the already mentioned references and it was depicted in the first part of this work. It could be a good general strategy in the sense that it has been defined by physical reasoning related to the differences in the flow structure between simple shear and detached flows.

#### 3.1. Turbulence: Eddy Viscosity Models (EVMs) selected

The followed methodology allows to select the SST  $k-\omega$ , (SST), EVM from Menter et al., 1994 and Menter et al., 2003, and the SST  $k-\omega$  with a Scale Adapted Simulation submodel, (SAS-SST) from Egorov et al., 2010 and Menter et al., 2010. The SST model is a Two-Equation model, where the mixture turbulent viscosity,  $\mu_{t,m}$  is computed by a combination of two variables representing the turbulence scales: the turbulent kinetic energy  $k$ , and its rate of dissipation  $\omega$ . They are computed by transport equations, TEQs, including the transport effects for each variable (i.e., the local and the convective variable accelerations, production, diffusion, dissipation, and source terms). In the TEQ for  $\omega$  there is also a damped cross-diffusion term,  $D_\omega$ , distinctive of the SST model when it is compared against the Standard  $k-\omega$  model (Versteeg et al., 2007). The SST model is based on the blending between the Standard  $k-\omega$  and the Standard  $k-\varepsilon$  models, transforming the Standard  $k-\varepsilon$  model in equations based on  $k$  and  $\omega$  which leads to the  $D_\omega$  term introduction.

The SAS-SST model is an improved URAS/EVM formulation, which allows the resolution of the turbulence spectrum in transient flow conditions. Contrary to the standard URAS/EVMs the SAS option provides two independent scales for the source terms of the underlying two equations model, (e.g., SST, Standard  $k-\omega$  or Standard  $k-\varepsilon$  models). In addition to the standard input for the length scale, i.e., the velocity gradient tensor  $\partial U_i/\partial x_j$ , SAS model computes a second length scale, called the von Karman length-scale,  $L_{vK}$  from the second derivative of the mean velocity field. The information provided by  $L_{vK}$  allows to react more dynamically to capture scales in the flow field which cannot be handled by standard URAS/EVMs. These formulations recover only the large-scale unsteadiness, whereas the SAS model adjusts to the already resolved scales in a dynamic way and could allow the development of a turbulent spectrum in the detached regions. Thus, SAS covers steady state regions (computed normally by RAS/EVMs) as well as unsteady detached flow regions (which must be computed by LES to solve their details) without an explicit switch in the model formulation. Then, SAS would allow URAS flow studies including a technique for adapting the length scales automatically instead of the more expensive LES option in terms of CPU requirements. The functionality of SAS is like the Detached Eddy Simulations, DES, being it a hybrid formulation that uses both EVMs and LES. The LES activity in DES is enforced by the grid limiter, whereas SAS allows a breakdown of the large unsteady structures by adapting the EVM to the locally resolved length scale. This functionality could be explored more extensively to open the possibility to perform URAS/EVM CFD with affordable CPU costs, see full details in [Egorov et al., 2010](#) and [Menter et al., 2010](#).

### 3.2. Two-phase/cavitating flow: Transport Equation-based Modeling (TEM) selected

The TEMs consist in solving a transport equation for either mass or volume fraction with appropriate source terms to regulate the mass transfer between phases. Like in the first part of this work, the [Singhal et al., 2002](#) model was used, because it showed a good performance in cases of cavitating flow in nozzles in previous works. It was already commented that the assessed TEMs were less sensitive to calibration than the EVM ones, ([Coussirat 2016-2021](#)), despite that it is necessary to consider in this TEM the turbulent pressure fluctuations computation and its related calibration. The original calibration from [Singhal et al., 2002](#) was used under an assumption of isotropy (from these authors) in the turbulence despite that in the boundary layer the turbulence is anisotropic. It is remarked that it is necessary to compute previously a suitable  $k$  level in the cavitation zone for a subsequent appropriate pressure field (mean + fluctuations) prediction under slightly or fully developed cavitation conditions. This fact led to pay more attention in the EVMs calibration than in the TEMs ones now.

### 3.3. Geometry, Boundary Conditions and Discretization Schemes Defined

The same considerations like in the first part of this work were made concerning to: 1) the CFD code used ([Ansys, 2018](#)), the defined mesh (two-dimensional, structured, 50,000 cells over the nozzle geometry, see [Fig. 1](#) and [Fig. 2](#)) and the grid sensitivity study performed (independence of the obtained results to the defined cell size, negligible 3D effects in the flow over its middle plane).

Also, the boundary conditions and the discretization schemes used were the same as the ones defined in the first part of the work, but they are briefly commented again. For the inlet boundary condition, a mean value for the  $c_{m,in}$  computed from the mass conservation principle, due to the inlet/outlet geometry sections and the  $c_{m,out} = f(\sigma)$  are known in advance. At the outlet, a  $p_{out}$  value was imposed ( $=1.0 \times 10^5$  Pa) and a non-slip condition was defined at the walls. The turbulence inlet/outlet boundary conditions were computed from standard formulations for  $k$  and  $\omega$ . The selected discretization schemes were: QUICK, for  $\rho$  and  $\nu f$ ; Least Squares Cell based, for the Gradients in the spatial discretization; Bounded Central Differencing, for the momentum

discretization; PRESTO, for pressure and SIMPLEC, for pressure-velocity coupling (Versteeg et al., 2007, Ansys 2018).

The 2D URAS/EVM simulations were performed for slightly developed ( $\sigma=1.19$ ) and fully developed ( $\sigma=0.94$ ) cavitation states, using the SST and the SAS-SST models. For each case its corresponding  $\sigma$  (or K) value was verified after each CFD modeling, by using the predicted inlet pressure  $p_{in}$  to compute them. The timestep was estimated from the Sr number range reported by Stanley et al. 2011, (i.e.,  $0.3 < Sr < 0.53$ ), and using the Eq. 1 for its computation. The necessary data for the timesteps computation were extracted from: 1) The Biçer 2015 database for the outlet velocity,  $c_{m,out}$  and 2) From Fig. 1 for the cavity length,  $L_{cav}$ . The computed values for  $c_{m,out}$  were 12.75 m/s and 14.35m/s for  $\sigma = 1.19$  and  $\sigma = 0.94$  respectively; and a value for the  $L_{cav}=0.5L_n = 0.004$  m was assumed. The computed shedding frequencies,  $f_{vs}$ , values were in the range 0.25 kHz  $< f_{vs} < 4.0$  kHz, then, the oscillation period was  $0.4 \times 10^{-3} \text{ s} < t_p < 2.5 \times 10^{-4} \text{ s}$ . Thus, the timestep defined must be of an  $O(\sim 5.0 \times 10^{-5})$  to avoid any numerical aliasing phenomena in the predicted  $f_{vs}$ . In the Bounded Second Order Implicit scheme a maximum of 50 iterations by timestep was sufficient to obtain convergence in each timestep during the transient simulation (Ansys 2018).

#### 4. CFD SIMULATIONS OF SLIGHTLY/FULLY DEVELOPED CAVITATION

Firstly, a RAS/EVM CFD was again carried out for slightly developed cavitation,  $\sigma=1.19$ , using the SST model performing a detailed calibration of the  $\beta^*$  parameter. Both the  $k$  production and its dissipation levels computed by the  $k$ -TEQ in the SST model are related to  $\beta^*$ . Its tuning allowed the improvement in the  $c_m$  and  $c'_{RMS}$  fields predictions leading to a more accurate cavity shape estimation. During the calibration it was observed that the  $c'_{RMS}$  field predicted was strongly affected, but the  $c_m$  field almost did not change (see details in the first part of this work). This fact remarks the close relation between the computed  $k$  level and the cavitation state predicted because it was checked that suppressing the  $v_{t,m}$  level by calibration the  $\nu_f$  predicted rises. Then, it is not sufficient to obtain only accurate values for the  $c_m$  field for an accurate cavitating flows CFD. It was demonstrated that by means of a careful calibration a RAS/EVM simulation is still possible at  $\sigma = 1.19$  (Coussirat et al., 2021). The obtained results from this RAS/EVM simulation (two/three-days/CPU Intel/CoreTM, i5-1.60G Hz, 8CPUs, ~1.8GHz-12GB/RAM) was compared against ones obtained by LES (SGS models from Smagorinsky and Vreman, computed by a Linux computer, 3.0 GHz  $\times$  32 cores, 16 CPU and 64GB RAM/node) using timesteps of  $O(10^{-8} \text{ s})$ , about 700,000 cells for a precursor simulation to obtain an inlet boundary condition, (three-weeks/CPU) and 2,800,000 cells in the nozzle simulations (one-week/CPU), see full details in Sou et al., 2014 and Biçer 2015.

The main conclusion here was that the obtained results using a calibrated EVM showed similar quality as LES ones but avoiding intensive CPU requirements. Fig. 2 shows the general shape of the cavity predicted by SST when  $\beta^*$  is changed. It was shown that depending on the selected  $\beta^*$  value, the  $v_{t,m}$  was suppressed in the detached flow zone leading to a rising in the  $\nu_f$ . The unsteady nature of cavitation in this case was captured despite the RAS/EVM simulation performed, because a ‘incipient shedding’ is observed, but without any physical sense (this shedding is like that one that appears in the flow around a cylinder when it is modelled by a steady state simulation as was reported by Ali et al., 2009).

The present URAS/EVM simulations try to solve this fact applying the previously developed calibration methodology. The cavity structures and its shedding for  $\sigma = 1.19$  were computed and compared against the experimental information available, see Fig. 3. Unfortunately, in the experiments there are no  $\nu_f$  level measurements in the cavity nor sequences of pictures showing shedding vortex. Only pictures of its ‘mean shape’ and some information related to the  $f_{vs}$  are

available for comparisons against the CFD results, (see full details in the Section. 2 in the first part of this work). To compare results showed in Fig. 3 against the previous steady case already presented in the first part of this work, the Fig. 2 has two different cavity  $\nu f$  scales for  $\beta^*_{\infty} = 0.18$ .

Notice that in Fig. 2 a maximum  $\nu f$  level of  $O(\sim 0.25)$  was predicted by the SST for this  $\beta^*_{\infty}$  value, but under a RAS/EVM simulation. On the other hand, Fig. 3 clearly shows the vortex shedding related to the  $\nu f$  rising in the cavity. Both the SST and the SAS-SST models were used here. These results are compared against experimental high-speed images from Bicer et al., 2014, Bicer 2015, and the RAS/EVM CFD results from Coussirat et al., 2021. Due to this lack of  $\nu f$  data in these experiments, a  $\nu f$  level of  $O(\sim 1)$  was assumed for the visualised experimental cavity, remarking that an exact  $\nu f$  level comparison against CFD results could not be carried out. Fig. 3 shows the low  $\nu f$  level computed by the URAS/SST model despite the calibrated  $\beta^*_{\infty}$ , and it is similar the one computed by means of RAS/EVM, Fig. 2, but a real shedding cycle is observed now due to the URAS simulation. Moreover, the URAS/SAS-SST model predicts higher  $\nu f$  levels and provoking a better-defined shedding cycle for the optimized  $\beta^*_{\infty}$  value.

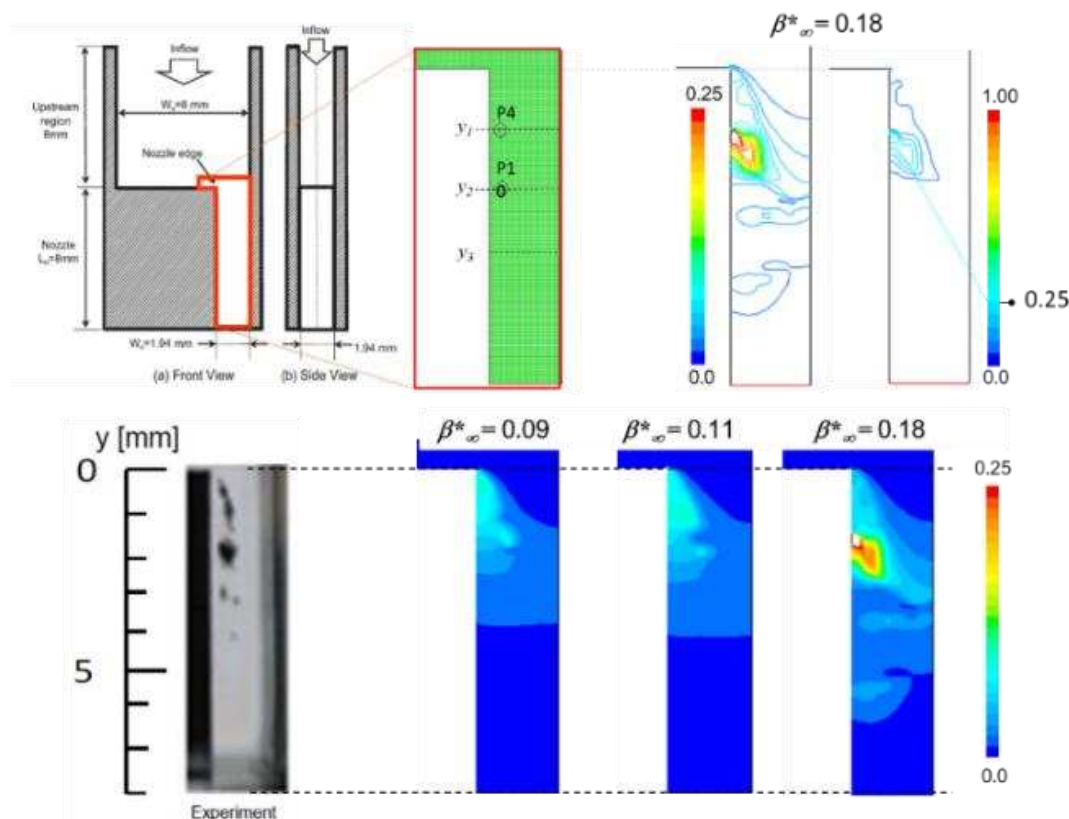


**Figure 2:** Top: Geometry, M03 mesh and RAS/EVM CFD results (SST model,  $\sigma = 1.19$ , steady state cavity shape and  $\nu f$  levels,  $\beta^*_{\infty} = 0.18$ ). Bottom: RAS/EVM CFD Sensitivity study for  $\beta^*_{\infty}$ . Notation: Exp., Experiments Sou et al., 2014; Red frame, measurement/CFD domain;  $\beta^*_{\infty}$ , calibration parameter.

The  $f_{\nu s}$  for the predicted Pressure Power Spectral Density (PPSD) signals at positions P4 and P10 were computed by a Fast Fourier Transform, Fig. 2. The shedding  $f_{\nu s}$  first mode computed by the SST model has a 500 Hz value and the  $f_{\nu s}$  second mode has 1,000 Hz, see Fig. 4. The peaks of the computed PPSD are at the same  $f_{\nu s}$  values in both stations, being their intensity different in both stations solely. The obtained  $f_{\nu s}$  values are similar as the ones reported in cavitating flow in nozzles by Sato et al., 2002, Stanley et al., 2011, De Giorgi et al., 2013 and Sou et al., 2014, (see details also in the first part of this work, Section 2).

The SST-SAS model predicts a more random PPDS signal without any clear peak, being the  $f_{vs}$  first mode computed now at  $\sim 200$  Hz. This result could be due to the SAS modelling strategy, related to the  $L_{vK}$  scale defined to activate the flow turbulence unsteadiness quickly.

Preliminary results by means of URAS/EVM simulation for  $\sigma = 0.94$  using both the SST and SAS-SST models, see Fig. 5 were compared against experimental high-speed images and LES simulations from Bicer et al., 2014 and Bicer 2015. Like in the former  $\sigma = 1.19$  case an exact  $\nu f$  level intercomparison could not be performed due to the lack of information. Assuming again  $\nu f$  levels of  $O(1)$  for the  $\nu f$  in the cavity, a low  $\nu f$  level was computed by the SST model, despite that the modified  $\beta^*_{\infty}$  value was set. On the other hand, the SAS model predicts higher  $\nu f$  levels as experiments apparently show. Like the former case ( $\sigma = 1.19$ ), the computed cavity has more complex structures when the SAS-SST model was used, but they look quite different that the ones obtained by LES, showing less ‘fine structures’ in the cavities convected downstream.

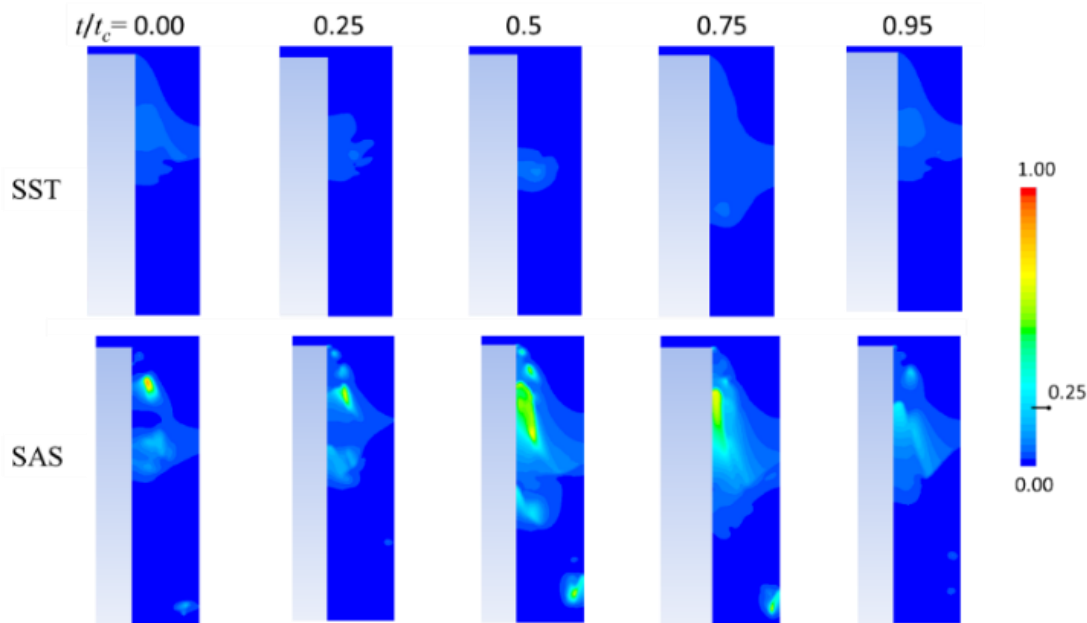


**Figure.3:** URAS/EVM CFD results (Transient case,  $\sigma = 1.19$ ,  $\beta^*_{\infty} = 0.18$ ): Cavity shape and  $\nu f$  evolution for one shedding cycle. Top: SST model. Bottom: SAS-SST model. Notation:  $t$  = timestep,  $t_c$  = complete cycle time.

Compared to the former case ( $\sigma = 1.19$ ) the  $f_{vs}$  first mode predicted by SST and by the SAS-SST has a lower value. More harmonics appear because a bigger cavity was predicted having more complex structures as experiments from Sato et al., 2002 show. The  $f_{vs}$  first mode predicted by the SST and SAS-SST was now  $\sim 400$  Hz ( $t_c = 2.5 \times 10^{-3}$  s) and 200 Hz ( $5.0 \times 10^{-3}$  s) respectively.

This shift to lower  $f_{vs}$  first mode values could be justified by the observed changes in the cavity evolution, because a bigger cavity has a more inertial behavior. In this way the vortex shedding due to the detachment of bigger cavities could be the reason for the shift to lower values for the  $f_{vs}$  first mode peak, despite that several and higher harmonics also appear, perhaps related to the more complex cavity dynamics. Unfortunately, in the Sou et al, 2014 and Bicer 2015 databases there are no experimental data nor ones computed by LES simulations related to the observed shedding frequencies.

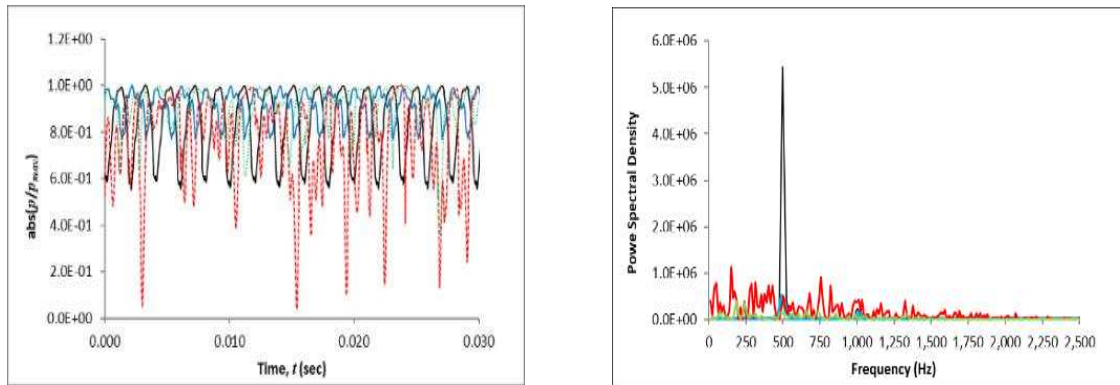


**Figure 4:** CFD results (URAS/EVM case,  $\sigma = 1.19$ ,  $\beta^*_{\infty} = 0.18$ ): Left: Pressure fluctuations at P4 and P10 stations, see Fig. 2. Right: PSD computed (Fast Fourier Transform, FFT) for P4 and P10. Computed frequency (first mode): SST= 500Hz ; SST-SAS = ~200Hz. Notation: SST: (Black, P4; Blue, P10); SST-SAS: (Red, P4 ; Green, P10).

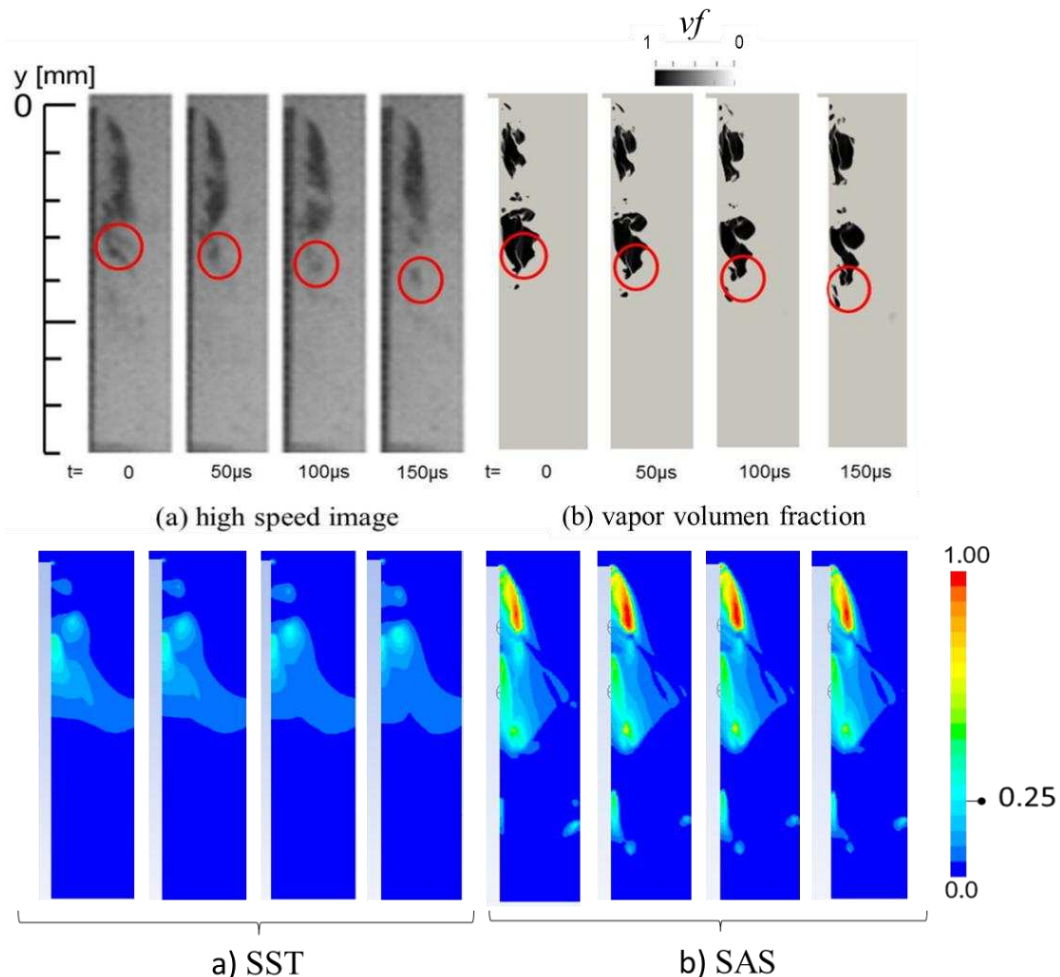


**Figure 5:** URAS/EVM CFD results (Transient case,  $\sigma = 0.94$ ,  $\beta^*_{\infty} = 0.18$ ): Cavity shape and  $vf$  evolution during a shedding cycle. Top Experiments, (a) high speed images and (b) CFD LES modelling (Sou et al., 2014, Bicer 2015). Bottom: Present CFD results SST and SAS-SST models. Notation:  $t$  = timestep,  $vf$  = vapor fraction.

## 5. CONCLUSIONS

A numerical study of developed cavitating flow in asymmetrical nozzle of injectors/atomizers by means of URAS/EVM simulations were carried out using calibrated SST and SAS-SST models. Both the cavity shape and the vortex shedding frequencies were obtained by these two models for slightly developed cavitation ( $\sigma = 1.19$ ) and fully developed cavitation ( $\sigma = 0.94$ ) cases. Assuming a  $O(\sim 1)$   $\nu f$  level in the cavity from the experiments, this was underestimated by the calibrated SST model. On the other hand, the SAS-SST model gives  $\nu f$  levels nearer to the experimental ones.

The  $f_{\nu s}$  first mode predicted by the SST model are like ones obtained in experiments and in CFD/LES simulations by several authors for  $\sigma = 1.19$ . These results allow concluding that there is a clear relation between the vortex shedding structure due to the  $k$  level predicted and the subsequent pressure field computed, leading to a more complex cavity behavior including vortex shedding. Despite that some preliminary results were obtained, more experimental information related to the  $\nu f$  level in the cavity is necessary for a detailed SST and SAS-SST calibration to predict both the cavity  $\nu f$  distribution, the cavity dynamics and the  $f_{\nu s}$  frequencies for fully developed cavitation.

## ACKNOWLEDGEMENTS

This current work was partially supported by the Universidad Tecnológica Nacional (UTN) within its own research programme (UTN/SCTyP). Authors would like to express their appreciation to the UTN for providing financial support for this study (research project UTI4905TC).

## REFERENCES

- Ali M., Doolan C., Wheatley V., Convergence Study for a Two-Dimensional Simulation of Flow Around a Square Cylinder at a Low Reynolds Number, *7th Int.Conf. on CFD in the Minerals and Proc.Industr. CSIRO*, Australia, 2009.
- Ansys/Fluent Software, 2020, <http://www.ansys.com/Industries/Academic/Tools/v15Tutorial>.
- Biçer B., Num. Simul. of Cavitation Phenomena inside Fuel Injector Nozzles, *PhD Thesis, Kobe Univ. Japan*, 2015.
- Coussirat, M., Moll, F., Cappa, F., and Fontanals A., Study of Available Turbulence and Cavitation Models to Reproduce Flow Patterns in Confined Flows,” *J. Fluids Eng.*, 138(9), 2016.
- Coussirat M., Moll F. and Fontanals A., Reproduction of the cavitating flows patterns in several nozzle geometries using calibrated turbulence and cavitation models, *Mec. Computac., Vol XXXV:819–841*, 2017.
- Coussirat, M., Moll, F., Recalibration of Eddy Viscosity Models for Numerical Simulation of Cavitating Flow Patterns in Low Pressure Nozzle Injectors. *J. of Fluids Engineering*, 143(3), 031503, 2021.
- De Giorgi, M. G., Ficarella A., and Tarantino M., Evaluating cavitation regimes in an internal orifice at different temperatures using frequency analysis and visualization. *Int.J. Heat and Fluid Flow* 39, pp160-172, 2013.
- Egorov, Y., Menter, F., Lechner, R., and Cokljat, D., The Scale-Adaptive Simulation Method for Unsteady Turbulent Flow Predictions—Part 2: Application to Complex Flows, *Flow Turb. Combust.*, 85(1), pp.139–165, 2010.
- Menter F., ‘Two Equations Eddy-Viscosity Turb. Models for Eng. Appl.’, *AIAA J.*, 32(8), pp. 1598–1605, 1994.

- Menter, F., and Egorov, Y., 'The Scale-Adaptive Simulation Method for Unsteady Turbulent Flow Predictions—Part 1: Theory and Model Description,' *Flow Turb. Combust.*, 85(1), pp. 113–138, 2010.
- Menter, F., Kuntz, M., and Langtry, R., 'Ten Years of Industrial Experience With the SST Turbulence Model,' *Turb., Heat and Mass Transfer*, Vol.4, K. Hanjalic, et al., eds., House, pp. 625–630, 2003.
- Sato, K., Saito, Y., Unstable cavitation behavior in a circular-cylindrical orifice flow. *JSME Int.J. Series B Fluids and Thermal Engineering*, 45(3), pp638-645, 2002.
- Sou A., Biçer B., Tomiyama A., Num. simulation of incipient cavitating flow in a nozzle of fuel injector, *Comp&Fluids* 103: pp42–48, 2014.
- Singhal, A., Athavale, M., Li, H., and Jiang, Y., Math. Basis and Validation of Full Cavitation Model, *J. Fluids Eng.* 124(3): pp617–624, 2002.
- Stanley, C., Barber, T., Milton, B., & Rosengarten, G., Periodic cavitation shedding in a cylindrical orifice. *Exp. in fluids*, 51(5), pp1189-1200, 2011.
- Versteeg H. and Malalasekera W., 2007, 'An Introduction to Computational Fluid Dynamics: The Finite Volume Method,' 2<sup>nd</sup> Ed., Upper Saddle River, NJ, USA, Pearson Prentice Hall; 2007.